Heat Extraction Capacity and Its Attenuation of Deep Borehole Heat Exchanger Array

Fangfang Zhang [a], Mingzhi Yu [a,b,*], Bjørn R Sørensen [c], Ping Cui [a], Wenke Zhang [a], Zhaohong Fang [a]

a. School of Thermal Engineering, Shandong Jianzhu University, Jinan, Shandong, 250101, China

b. The Co-Innovation Center for Green Building of Shandong Province, Jinan, Shandong, 250101, China

c. Department of building, Energy and Material Technology, UiT The Arctic University of Norway, N-8514, Norway

Abstract: A model is proposed to analyze the heat transfer of deep borehole heat exchanger (DBHE)arrays. Based on this, a dimension reduction algorithm is proposed for the numerical simulation of heat transfer of DBHE arrays, which can improve calculation speed by several orders of magnitude compared with that by the CFD software. An index of heat extraction capacity (HECI) is adopted to evaluate the heat extraction capacity of DBHE arrays. The influence of borehole spacing, operation time, annual heating duration, terrestrial heat flow rate, borehole depth, soil thermal parameters, pipe diameter and circulating fluid flow rate on DBHE array heat extraction capacity and its attenuation are analyzed. The results show that the borehole spacing, operation time, and annual heating duration all have apparent influence on DBHE array heat extraction capacity and its attenuation rate, while the others only have apparent influence on the heat extraction capacity. According to the calculation results, when the DBHE arrays have a service lifetime of 20 to 50 years, the recommended borehole spacing range is 40 to 70 m.

Keywords: Deep borehole heat exchanger array, Heat transfer model, Numerical simulation, Heat extraction capacity, Attenuation of heat extraction capacity

Nomenclature	
a	thermal diffusivity (m^2/s)
c	specific heat (J/(kg·K))
C	pipe heat capacity per linear meter (J/(m·K))
H	borehole depth (m)
M	fluid flow rate (kg/s)
n	number of boreholes
Q	HECI of DBHE (kW)
q	heat flow (W/m^2)
R	thermal resistance (m·K/W)
r	radial coordinate (m)
T	soil temperature (°C)
x	x coordinate (m)
y	y coordinate (m)
z	axial coordinate (m)
Greek	
λ	thermal conductivity (W/(m·K))
θ	excess temperature (°C)

* Corresponding author
Email Address: yumingzhiwh@163.com

τ	time (s)
ζ	attenuation rate of the HECI (%)
$\Delta\zeta$	annual HECI attenuation rate (%)
ΔHECI	the change rate of HECI with the variation of borehole spacing (%)
Subscripts	
0	initial
1	outer pipe
1st	the first year
2	inner pipe
b	borehole wall
f	fluid
f_1	fluid in the annular channel
f_2	fluid in the inner pipe
fp	per borehole
g	ground, terrestrial
i, j	sequential number of borehole
k	sequential number of strata
L	the total number of strata involved
load	the load of DBHE
n	the *n*th
n-1	the (*n*-1)th
s	single-borehole

1. Introduction

Compared with shallow ground source heat pumps (SGSHPs), deep ground source heat pumps (DSGHPs) have much larger capacity to meet heating demand with less land demand [1] for their deep borehole heat exchangers (DBHEs) usually have depth of 2000-3000 m which are much deeper than that of SGSHPs and involve much hotter soil. In recent years, more and more DGSHPs have been applied [2,3]. Due to the very deep size and the complex geotechnical conditions involved, it is not an easy task to analyze heat transfer of DBHE. Until now, how to fast calculate or simulate DBHEs, especially DBHE arrays, is still a difficult problem for researchers to face.

The heat transfer of DBHE can be generally solved by analytical [4-6] and numerical methods [7,8] Beier et al. proposed an analytical model to describe the heat transfer in coaxial borehole heat exchangers, but the model does not consider the geothermal gradient [6]. Analytical models proposed by Luo et al. consider the geothermal gradient but the calculation work is very heavy when consider the nonuniform heat flux along the borehole [4,5].

Because numerical method can adapt to complex geotechnical conditions, it has become an essential mean for heat transfer analysis of DBHE. FLUENT [7,8], OpenGeoSys [9,10], FEFLLOW [11,12] and other software have been used to study the heat transfer performance of DBHE. However, it is difficult to use the above softwares to simulate and analyze the whole life operation properties of DBHE due to the great number of space and time grids. Holmberg et al. [13], Fang et al. [14], Cai et al. [15] and Yu et al. [16] adopted different improved algorithms to solve the numerical models of single-borehole DBHE,

which could improve the calculation speed in different degrees. For a DBHE array has not only one borehole and usually has to be analyzed in three-dimensional rectangular coordinate system, the methods to improve the calculation efficiency for single-borehole DBHE which usually adopt in two-dimensional cylindrical coordinate system cannot be used directly.

Until now, only few research related to heat transfer of DBHE array has been reported. Deng et al. [17] and Li et al. [18] analyzed the operation performance of DBHE array in one heating season based on the experimental measurement data. Studies have shown that the performance of heat pump units and system comprehensive performance of the DGSHPs system are higher than that of the conventional SGSHPs. Because the projects have only operated for no more than two years, their long-term operation performance and heat extraction capacity are not clear. Cai et al. [9] established a numerical heat transfer model for a 5-borehole DBHE array in Xi 'an by the software of OpenGeoSys and analyzed the thermal influence among boreholes. The grid amount of the numerical model mentioned above was very large, and it took 143 hours to simulate a heating season operation on a high-performance workstation. Because the heat transfer analysis of DBHE array is usually a three-dimensional unsteady problem in Cartesian coordinates, it is an extremely difficult and time-consuming task to simulate the heat transfer of the whole life or even of only several years operation.

Liu et al. [19] found that the outlet fluid temperature decline rate of a single-borehole DBHE which has a constant heat extraction rate, increased from 9.66% to 19.12% during the running period of 30 years. The research of Ran et al. [20] showed that the geotechnical temperature around single-borehole DBHE and the outlet temperature of circulating liquid decreased year by year. From the above research, it can be concluded that the heat extraction capacity of DBHE decreases gradually due to soil temperature decrease, but the attenuate rate is still unknown.

The DBHE maximum heat extraction capacity (MHEC) is the constant thermal load that a DBHE undertakes when the inlet circulating fluid temperature reaches its lowest allowable value at the end of a certain operation period. MHEC can be used to evaluate the heat extraction ability of DBHEs and its variation with operation time. To determine the MHEC is an inverse heat transfer problem, which is obtained by iterative operation based on the heat transfer model of DBHE, the assumed inlet circulating fluid temperatures and other parameters. However, the calculation time of the inverse problem is greatly determined by the calculation speed of the DBHE heat transfer model. As mentioned above, heat transfer calculation of DBHE array is an extremely difficult and time-consuming task, thus to determine the MHEC by iterative calculation of DBHE array heat transfer model needs much more time.

To fast determine the MHEC of DBHE array, this paper proposed a dimension reduction algorithm for numerical simulation of the heat transfer of DBHE, which can cut down the calculation time by several magnitude orders.

2. Heat Transfer model

Soil temperature distribution and variation is the result jointly caused by heat transfer of all borehole heat exchangers (BHE) of a DBHE array. For one of the BHE, the heat transfer process of it can be divided into two parts, i.e. the heat transfer inside and outside the borehole. Therefore, the DBHE heat transfer model is composed of two sections as following.

2.1 The model outside the borehole

The following assumptions are adopted for heat transfer outside the borehole,

1) Ground water seepage is ignored and only heat conduction is considered;

2) Geological strata are horizontal and parallel to the ground surface, and the thermophysical properties of each stratum are uniform and maintains constant;

3) The terrestrial heat flux and the ground surface temperature maintain constant.

According to the above assumptions, the heat transfer outside the borehole is as in **Eqs.** (1)–(8):

$$\frac{1}{a}\frac{\partial T}{\partial \tau}=\frac{\partial^2 T}{\partial r^2}+\frac{1}{r}\frac{\partial T}{\partial r}+\frac{\partial^2 T}{\partial z^2},\quad r_{\mathrm{b}}\le r<\infty,0\le z<\infty,\tau\ge 0 \tag{1}$$

$$T=t_0,\qquad r_{\mathrm{b}}\le r<\infty,z=0,\tau\ge 0 \tag{2}$$

$$\frac{\partial T}{\partial z}=\frac{q_g}{\lambda_L},\qquad r_{\mathrm{b}}\le r<\infty,z\to\infty>>H,\tau\ge 0 \tag{3}$$

$$\frac{\partial T}{\partial r}=0,\qquad r\to\infty,0\le z<\infty,\tau\ge 0 \tag{4}$$

$$T=T_{\mathrm{b}},\qquad r=r_{\mathrm{b}},0\le z\le H,\tau\ge 0 \tag{5}$$

$$-2\pi\lambda_{\mathrm{k}} r\frac{\partial T}{\partial r}=\frac{T_{\mathrm{f1}}-T_{\mathrm{b}}}{R_1},\qquad r=r_{\mathrm{b}},0\le z\le H,\tau\ge 0,\ k=1,2\cdots L \tag{6}$$

$$\frac{\partial T}{\partial r}=0,\qquad r=r_{\mathrm{b}},H<z<\infty,\tau\ge 0 \tag{7}$$

$$\begin{cases} T_0=t_0+\dfrac{q_g}{\lambda_L}\left(z-z_{L-1}\right),\quad 0<z<\infty,\ r_{\mathrm{b}}\le r<\infty,\tau=0,L=1 \\ T_0=t_0+\displaystyle\sum_{k=1}^{L-1}\frac{q_g}{\lambda_{\mathrm{k}}}\left(z_k-z_{k\text{-}1}\right)+\frac{q_g}{\lambda_L}\left(z-z_{L-1}\right),\quad 0\le z_{L-1}<z\le z_L<\infty,\ r_{\mathrm{b}}\le r<\infty,\tau=0,L=2\cdots N \end{cases} \tag{8}$$

Where, a is the thermal diffusivity of soil, m^2/s; T is the temperature of soil/rock, ℃; τ is time，s; r is the radial coordinate, m; z is the depth coordinate，m; r_{b} is the borehole radius, m; t_0 is the initial surface temperature, ℃; q_{g} is the terrestrial heat flow rate, W/m^2; λ is the thermal conductivity of soil/rock, W/(m·K); H is the borehole depth，m; T_{b} is the borehole wall temperature, ℃; T_{fl} is the inlet fluid temperature, ℃； R_1 is the thermal resistance between the fluid in the annular channel and borehole wall, m·K/W; T_0 is the initial soil temperature, ℃; L is the total number of strata involved.

The authors' previous studies have proved that [21] the superposition principle is still valid for the heat transfer problem of the DBHE array. Thus, the soil temperature is calculated by the following equation:

$$T\left(x,y,z,\tau\right)=\sum_{i=1}^{n}\theta_i\left(r_i,z,\tau\right)+T_0\left(r,z,\tau\right) \tag{9}$$

Where, T_0 is the initial soil temperature, and θ_i is the temperature response caused by of the ith borehole operation alone with the initial soil temperature of zero degree; x and y are the rectangular coordinates of a certain point on the horizontal plane; r_i is the distance between point (x,y) and the ith

borehole axis in the given horizontal plane and can be calculated by the following equation,

$$r_i = \sqrt{(x - x_i)^2 + (y - y_i)^2} \tag{10}$$

Where x_i, y_i are the rectangular coordinates of the ith borehole on the plane, respectively, m.

2.2 The model inside the borehole

The following assumptions are adopted for heat transfer inside the borehole,

1）The buried pipe is coaxial and the fluid velocity distribution and temperature distribution of the horizontal cross-section are both uniform；

2）The axial heat conduction of the solid phase inside the borehole is ignored；

3）The fluid in the outside annular channel flows downward and that in the inner pipe is upward.

Based on the above assumption, the inlet and outlet fluid temperature T_{f1} and T_{f2} can be obtained by **Eq. (11)**.

$$\left.\begin{aligned} C_1 \frac{\partial T_{f1}}{\partial \tau} &= \frac{T_{f2} - T_{f1}}{R_{12}} + \frac{T_b - T_{f1}}{R_1} - Mc \frac{\partial T_{f1}}{\partial z} \\ C_2 \frac{\partial T_{f2}}{\partial \tau} &= \frac{T_{f1} - T_{f2}}{R_{12}} + Mc \frac{\partial T_{f2}}{\partial z} \end{aligned}\right\}, \qquad (0 \le z \le H) \tag{11}$$

Where, C_1 and C_2 are the heat capacity of outer and inner pipe segments per unit length respectively, J/(m·K); c is the specific heat of fluid, J/(kg·K); M is the mass flow rate of the fluid in the coaxial pipe, kg/s; R_{12} is the thermal resistance between the two streams of circulating fluid, m·K/W.

T_{f1} and T_{f2} satisfy:

$$T_{f1} = T_{f2}, \qquad (z = H) \tag{12}$$

$$T_{f1} - T_{f2} = \frac{q_{load}}{Mc}, \qquad (z = 0) \tag{13}$$

where q_{load} is the heat extraction load, kW.

The borehole wall temperature meets the following conditions:

$$-2\pi\lambda_k r \frac{\partial \theta}{\partial r} = \frac{T_{f1} - T_b}{R_1}, \qquad (r = r_b, 0 \le z \le H, \tau \ge 0) \tag{14}$$

$$T_b = \theta_j(r_b, z, \tau) + \sum_{i=1}^{n, i \ne j} \theta_i(r_{ij}, z, \tau) + T_0(z, \tau) \tag{15}$$

Where $\theta_j(r_b, z, \tau)$ is the jth borehole wall temperature response with the initial soil temperature of zero degree, ℃; $\theta_i(r_{ij}, z, \tau)$ is the jth borehole wall temperature response induced by the ith borehole with the initial soil temperature of zero degree, ℃;. r_{ij} can be calculated by **Eq. (16)**.

$$r_{ij} = \sqrt{(x_i - x_j)^2 + (y_i - y_j)^2} \tag{16}$$

Where, x_j, y_j are the rectangular coordinates of the jth borehole on the plane, respectively, m.

The above calculation method based on the superposition principle decomposes the complex three-dimensional unsteady heat conduction model of DBHE array into the superposition of some two-dimensional single-borehole DBHE problems in cylindrical coordinates, which can greatly improve the solving speed of DBHE array heat transfer problem. Therefore, it is possible to simulate and calculate

the inverse problem of heat transfer process by using the above dimension reduction algorithm for DBHE array, which provides a feasible tool for quantitatively evaluating the heat extraction capacity of DBHE array and attenuation characteristics of heat extraction capacity.

2.3 Model validation

The CFD software of FLUENT was used to verify the proposed DBHE array heat transfer model. To lessen the calculation burden of FLUENT, the case analyzed adopts a small scale DBHE array of two boreholes which are 20m apart and 1000m deep. The meshing of the FLUENT model is shown in **Fig. 1**. The borehole diameter is 0.26 m, the terrestrial heat flow rate is 0.075 W/m^2, the ground surface temperature is 15℃, soil thermal conductivity is 2.5 W/(m·K), soil volumetric heat capacity is 2.4×10^6 J/(m^3·K), the circulating fluid flow rate is 6 kg/s and the heat extraction load is 100 kW per borehole. Other parameters are list in **Table 1**. The SIMPLE solver was selected for verification, the standardized k-epsilon turbulence model was selected for the fluid region, and the no-slip boundary condition was selected for the tube wall surface.

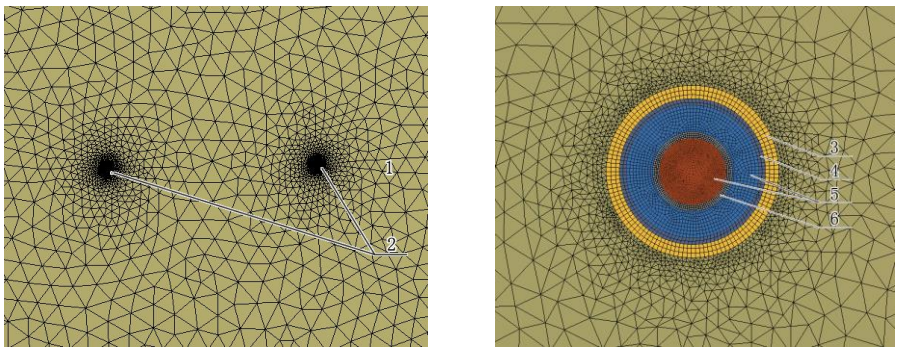

1—soil; 2—borehole; 3—grout; 4—outer pipe; 5—fluid; 6—inner pipe

(a) (b)

Fig. 1. Grid diagrams of (a) global DBHE cross section and (b) cross section of one borehole of a two-borehole DBHE.

Table 1 Parameters of the coaxial pipe and grout.

Parameter	Outer pipe	Inner pipe	Grout
Outer diameter(m)	0.2	0.1	——
Wall thickness (m)	0.005	0.005	——
Thermal conductivity (W/(m·K))	45.0	0.17	2.5
Volumetric heat capacity (J/(m^3·K))	2.1×10^6	1.6×10^6	0.8×10^6

Fig. 2 shows the inlet and outlet circulating fluid temperature variations calculated by the proposed model and FLUENT. The calculation results of the two models are in good agreement and the error ranges in (-0.2 ℃~ 0.29 ℃) during the simulated 4000 h operation period, which indicates that the calculation accuracy of the proposed model is similar as that of FLUENT. It took about 45 hours to execute calculation by FLUENT on an E5-2697V3 (memory 128G) workstation with the operation system of Windows 10, while only 3 seconds cost to complete the calculation by a notebook (i7-8565U CPU@1.8GHZ, memory 8G) with the proposed model. The calculation speed of the proposed model is increased by 5 orders of magnitude. Above results show that the proposed model can fast simulate the heat transfer of DBHE array with reliable calculation accuracy, which also means no more utmost

demands of computational hardware needed yet.

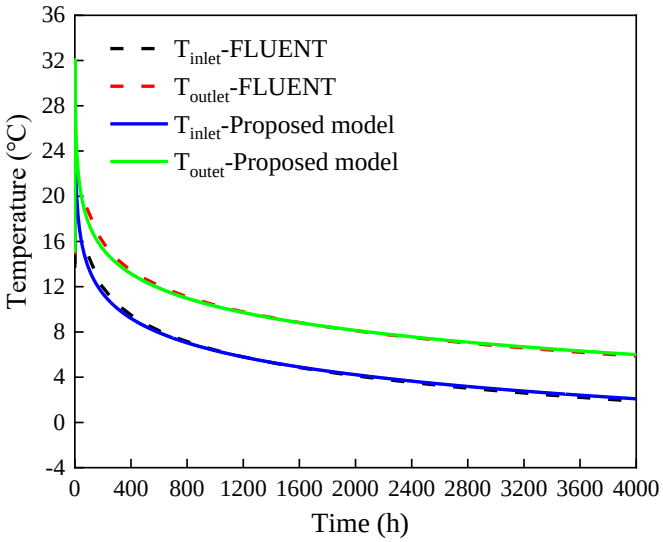

Fig. 2. The inlet and outlet fluid temperature calculated by the two models.

3. Parameters to evaluate heat extraction capacity and its attenuation

Heat extraction capacity greatly influences the operation of borehole heat exchangers [22-24], which is a key factor for designing DGSHP systems. Until now, there is no generally acceptable parameter to denote or evaluate the heat extraction capacity and its attenuation of a DBHE. Therefore, it is necessary to define a reasonable index to evaluate the heat extraction capacity of DBHE arrays. For heating systems are usually designed to ensure normal operation at the most adverse conditions, this paper proposes a HEC index (HECI) of DBHE arrays, which denotes each year's maximum constant HEC. The maximum constant HEC is the continuous constant heat extraction rate during whole heating seasons under the condition that the inlet fluid temperature gets to the lower limit which is 5 ℃ in this paper.

The DGSHPs system usually only extracts heat from soil with no heat recharge, which will inevitably cause the heat extraction capacity of the DBHE decline year by year. In order to clearly reveal the decline degree and regularity, the HECI attenuation is also analyzed in this section. The calculation flow chart is shown in **Fig. 3**. A parameter, ζ, is used to evaluate the HECI variation. Here, ζ is the attenuation rate of the HECI of the nth year compared with that of the first year, and it can be obtained by **Eq. (17)**:

$$\zeta = \frac{Q_{1st} - Q_n}{Q_{1st}} \tag{17}$$

Where, Q_{1st} and Q_n are the HECI of the first year and the nth year, kW, respectively.

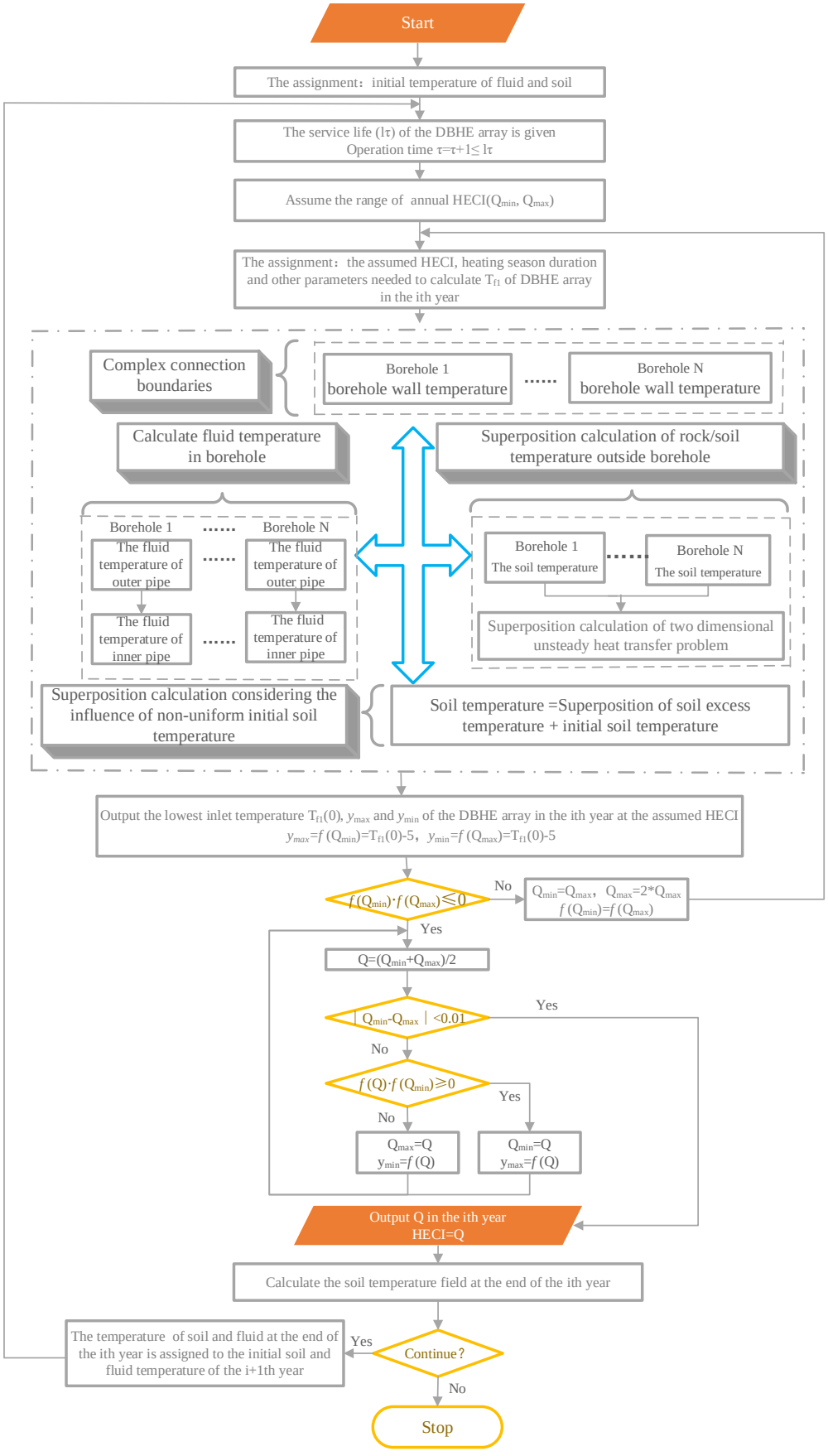

Fig. 3. The HECI calculation flow chart.

4. Calculation results and discussion of heat extraction capacity and its attenuation

In this section, a DBHE array of four boreholes arranged in square is used as the case to analyze the HECIs properties. The boreholes depth is 2000 m, the circulating liquid flow rate is 12 kg/s, the borehole diameter is 0.27 m, the terrestrial heat flow rate is 0.065 W/m^2, and the soil surface temperature is 15 ℃. The borehole parameters and soil physical parameters are shown in **Table 2** and **Table 3**.

Table 2 Parameters of boreholes.

Parameter	Outer pipe	Inner pipe	Grout
Outer diameter (mm)	193.7	110	——
Wall thickness (mm)	8.33	10	——
Thermal conductivity (W/(m·K))	45.00	0.40	1.5
Volumetric heat capacity (J/(m^3·K))	3.4×10^6	1.2×10^6	2.2×10^6

Table 3 Soil thermo-physical parameters.

Stratum (m)	Thermal conductivity (W/(m·K))	Volumetric heat capacity (J/ (m^3·K))
0 -500	1.50	2.36×10^6
500 -1000	2.00	2.38×10^6
1000 -1500	2.50	2.40×10^6
1500 -2200	3.00	2.42×10^6

4.1. Influence of borehole spacing on heat extraction capacity and its attenuation

When the heating load is not large, a single DBHE can meet the heating demand. But when the heating load is very large, a DBHE array with multiple boreholes is needed. According to studies of heat exchange properties of large shallow BHE, the borehole spacing has apparent influence on BHE heat exchange capacity [23,25], it can be inferred that borehole spacing probably is an important parameter affecting the heat extraction capacity of DBHE arrays. In this section, the DBHE array which draws heat for 4 months each year as the example to discuss the influence of borehole spacing on heat extraction capacity.

Fig. 4 shows the average borehole HECI variation of the four-borehole DBHE array with different borehole spacing and that of the single-borehole DBHE which borehole spacing can be seen as infinite. It can be seen from **Fig. 4** that the HECIs of the DBHE with the single-borehole and the four-borehole array arrangement are nearly same in the first three years, and their HECIs attenuate year by year during the 50 years' operation. The difference between the single-borehole and the DBHE array increases with operation time increases, and begins to decrease apparently with borehole spacing increasing since the fourth year. This is mainly because the heat extraction region involved is small in the first three years, and the influence of borehole spacing on the HECI is not obvious. With the increase of time, the influence of borehole spacing becomes obvious due to the expansion of the heat extraction region, and the HECI decreases due to the temperature decrease of soil adjacent to the borehole. The larger the heat extraction region a borehole involves, the more heat can be provided by soil during the heat extraction period.

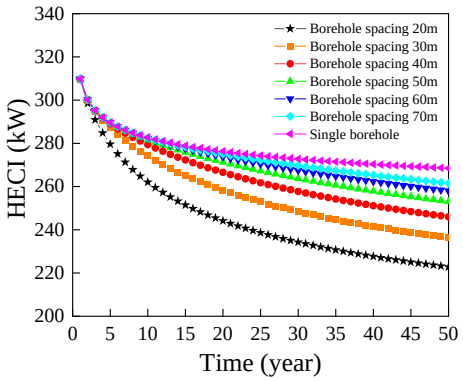

Fig. 4. HECI of the single and the four-borehole DBHE array.

Taking the HECI of the single-borehole with the same parameters as those of the four-borehole DBHE array as the reference, the change rate of HECI, i.e. ΔHECI, is defined to evaluate the heat extraction capacity decrease degree of the DBHE array compared with the single borehole. ΔHECI can be obtained by the following equation.

$$\Delta\mathrm{HECI}=\frac{Q_{\mathrm{fp}}-Q_{\mathrm{s}}}{Q_{\mathrm{s}}} \qquad (18)$$

Where, Q_{s} is the HECI of the single-borehole DBHE, kW; Q_{fp} is the average borehole HECI of DBHE arrays, kW.

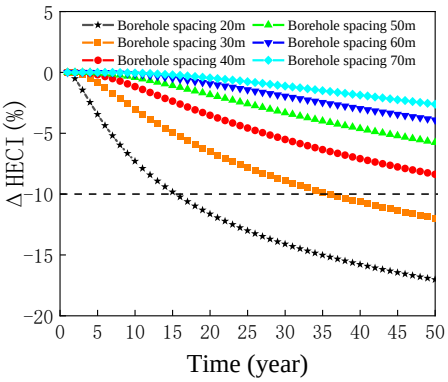

Fig. 5. ΔHECI of the four-borehole DBHE array with different borehole spacing.

ΔHECI calculated according to **Eq. (18)** is shown in **Fig. 5**. Obviously, the smaller the absolute value of ΔHECI is, the average borehole HECI of DBHE arrays is closer to that of the single-borehole. When the borehole spacings are 20 m, 30 m, 40 m, 50 m, 60 m and 70 m, the ΔHECI of the DBHE array ranges in (-11.64 % ~ -17.03 %), (-6.52 % ~ -11.98 %), (-3.52 % ~ -8.38 %), (-1.83 % ~ -5.76 %), (-0.93 % ~ -3.91 %) and (-0.45 % ~ -2.62 %) during the 20~50 year-operation periods, respectively. In the above calculation results, for the DBHE array with service lives of 20 to 50 years, the absolute values of ΔHECI are all less than 10% when borehole spacing is larger than 40 m. Therefore, in order to ensure the long-term heat extraction efficiency of DBHE, the borehole spacing should be appropriately increased.

Fig. 6(a) shows the influence of borehole spacing on the HECI attenuation rate(ζ) of the single-borehole DBHE and that of the four-borehole DBHE array. As shown in **Fig. 6**(a), the ζ of the DBHE array decreases with the borehole spacing increases, and the ζ of the single-borehole DBHE is always smaller than that of the DBHE array. The values of ζ of the DBHE array are 28.08 %, 23.71 %, 20.58 %, 18.31 %, 16.70 %, and 15.59 % after 50 years when the borehole spacing are 20 m, 30 m, 40 m, 50 m,

60 m, and 70 m respectively, while the ζ of the single-borehole DBHE is 13.32 %. The main reason is that thermal disturbance among boreholes decreases with the borehole spacing increases.

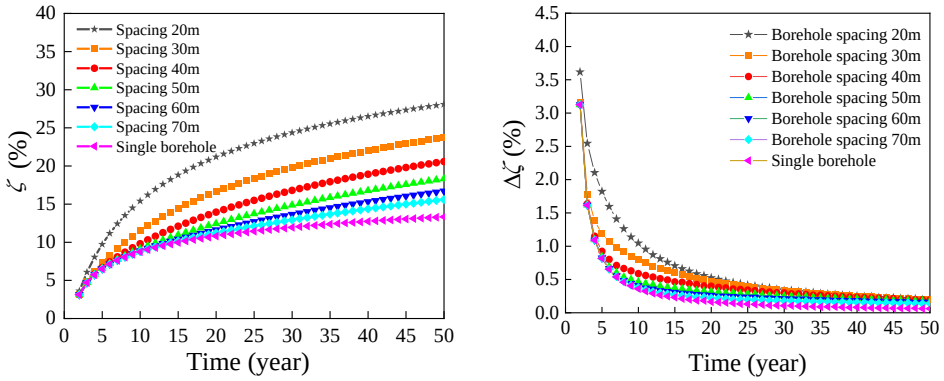

(a) (b)

Fig. 6. (a) ζ and (b) $\Delta\zeta$ of the single and the four-borehole DBHE array vs. time.

As shown in **Fig. 6**(a), the borehole spacing has great influence on ζ, and ζ increases continuously with time increases. To learn the ζ variation tendency with operation time increases, the annual HECI attenuation rate $\Delta\zeta$ is analyzed, which is the ratio of HECI of the nth year compared with that of the (n-1)th year. It can be obtained by **Eq. (19)**,

$$\Delta\zeta = \left| \frac{Q_n - Q_{n-1}}{Q_{n-1}} \right| \tag{19}$$

Where, Q_n and Q_{n-1} are the HECIs of the nth year and the (n-1)th year, KW, respectively.

Fig. 6(b) shows the $\Delta\zeta$ variation of the single-borehole DBHE and that of the four-borehole DBHE array. It indicates that, although the ζ increase year by year, the $\Delta\zeta$ gradually decreases and tends to zero with time increases. With different borehole spacings, the maximum $\Delta\zeta$ in the first two years can reach 3.62%, and $\Delta\zeta$ are all less than 0.34% and 0.20% after 30 years and 50 years, respectively. $\Delta\zeta$ of the single-borehole DBHE is 0.06% after 50 years. This indicates that the HECI of DBHE arrays tend to be stable after scores of years operation regardless borehole spacing.

4.2. Influence of annual heating duration on heat extraction capacity and its attenuation

Longer annual heating duration means more heat is extracted from soil during the heating period, which causes the underground temperature field recovery becoming more difficult during the non-operation period [15]. In order to study the influence of annual heating duration on heat extraction capacity of DBHE array, the following 3 modes are adopted according to annual heating duration. Mode 1: the annual run-stop ratio of heating time is 4:8; Mode 2: the annual run-stop ratio is 5:7 and Mode 3: the annual run-stop ratio is 6:6. In the three modes, the annual heating durations are 4 months, 5 months, and 6 months respectively, and the annual non-heating periods are 8 months, 7 months, and 6 months respectively.

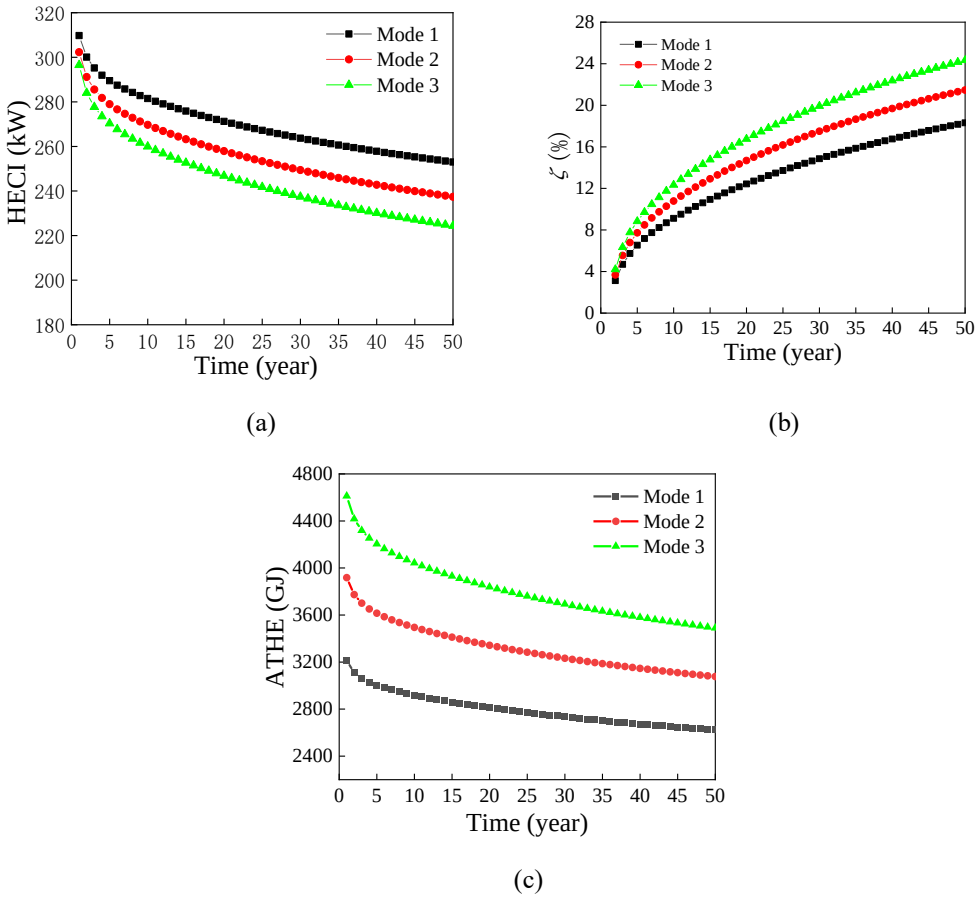

Fig. 7. Variation of (a) HECI, (b) ζ and (c) ATHE with different annual heating durations.

Fig. 7(a) shows the average borehole HECI variation of the DBHE array which borehole spacing is 50m. The average borehole HECI decreases with the annual heating duration increases. In the first year, the difference among the HECIs of the three modes are not much, and the difference of HECIs compared with each other of the three modes are all less than 5 %. However, with the increase of the operation time, the difference of HECI among the three modes gradually increases. The HECI of Mode 2 and Mode 3 are both smaller compared with that of Mode 1, and the differences between the Mode 1 and 2 and that between Mode 1 and 3 increase from 7.4 kW and 13.2 kW in the first year to 15.6 kW and 28.7 kW in the 50th year, individually. In Mode 1, the HECI of the four-borehole DBHE after 50 years is 9 % lower than that after 20 years. Compared to Mode 1, the HECI has an 11% reduction after 50 years in Mode 3. As well known, longer annual heating duration causes lower soil temperature at the end of each heating period, and then results in lower heat extraction capacity of the next heating period. Therefore, the difference of HECI among different modes increases with the increase of operation time.

Fig. 7(b) shows that the annual heating duration has apparent influence on HECI attenuation rate ζ, and longer annual heat duration induces larger ζ. For Modes 1, 2 and 3, the ζ after 50 years are 18.31 %, 21.46 % and 24.33 % respectively. As well known, longer annual heating duration means lower soil temperature and shorter annual thermal recovery time. Therefore, for DBHEs with same borehole spacing, the ζ of Mode 3 is significantly greater than those of Mode 1 and 2. **Fig. 7**(b) also indicates that the increase rates of ζ of all modes gradually become smaller with operation time increases, which means the $\Delta\zeta$ of the three modes decreases as time goes on. After 30 years, all $\Delta\zeta$ are all less than 0.35%.

Though Mode 2 and Mode 3 have larger HECI attenuation ζ compared with Mode 1, their annual total heat extractions (ATHEs) are larger than that of Mode 1 (see **Fig. 7**(c)). The ATHEs of Mode 2 and

Mode 3 are 22.00% and 43.59% larger than that of Mode1 in the first year, and are 17.29% and 33.00% in the fiftieth year, respectively. The reason is that longer annual heating duration provides more time to draw heat from the ground, which conduces to increase the ATHE.

4.3. Influence of terrestrial heat flow rate on heat extraction capacity and its attenuation

In this and following sections, the borehole spacing and DBHE annual run-stop ratio adopted are 50 m and 4:8, respectively. The terrestrial heat flow rate ranges in 0.03 W/m^2~ 0.09 W/m^2 which is suitable for most regions of China [26]. Other parameters are list in **Table 2** and **Table 3**. The calculated results are as follows.

Fig. 8(a) shows that the terrestrial heat flow rate has great influence on HECI and HECI increases with the increase of terrestrial heat flow rate and attenuates with time extension. Compared with the HECI with the terrestrial heat flow rate of 0.03 W/ m^2, the HECI improvements are 21.26± 0.03%, 42.52± 0.07%, 63.81± 0.10%, 85.07± 0.13%, 106.33±0.16% and 127.60±0.21% when the terrestrial heat flow rates are 0.04W/m^2, 0.05W/m^2, 0.06W/m^2, 0.07W/m^2, 0.08W/m^2 and 0.09W/m^2, respectively. The ground temperature gradient increases with the increase of the terrestrial heat flow rate, therefore the mean borehole wall temperature in the case of large terrestrial heat flow rate is larger than that of small terrestrial heat flow rate. As the result, the mean temperature difference between circulating fluid and borehole wall increases with terrestrial heat flow rate increases, which brings the increase of the HECI.

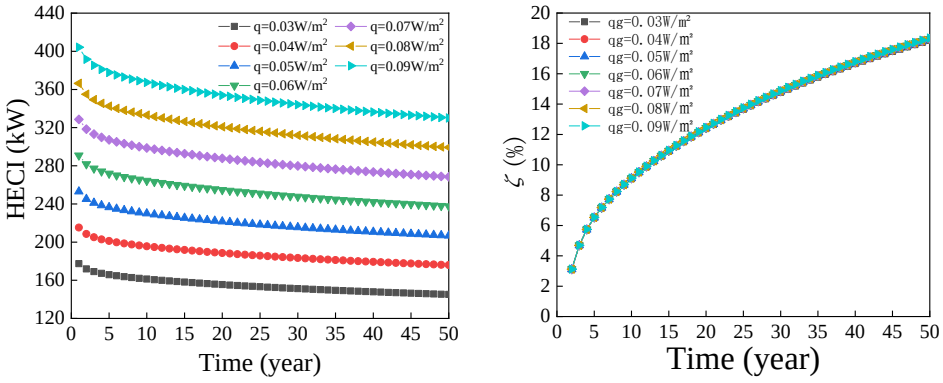

(a) (b)

Fig. 8. Variation of (a) HECI and (b) ζ with different terrestrial heat flow rates.

Fig. 8(b) shows the influence of terrestrial heat flow rate on the attenuation of HECI, i.e. ζ, is very weak. No matter how large the terrestrial heat flow rate is, the heat extraction capacity attenuation patterns of the DBHE array are nearly same. When the terrestrial heat flow rate ranges in 0.03 W/m^2 ~ 0.09 W/m^2, the change of ζ with different terrestrial heat flow rate are no more than 0.01 %, 0.03 %, 0.06 %, 1 0.06 %, 0.07 % after 10, 20, 30, 40 and 50 years, respectively. This indicates that when other conditions are constant, ζ is greatly affected by the operation time and hardly affected by the terrestrial heat flow rate.

4.4. Influence of borehole depth on heat extraction capacity and its attenuation

As shown in **Fig. 9**(a), the deeper the borehole is, the bigger the HECI is, and the HECI gradually attenuates with the increase of operating time. When the borehole depths are 1700 m, 1900 m, 2100 m, 2300 m and 2500 m, compared with the HECI of the DBHE with the depth of 1500 m, the HECI improvements during 50 years are 26.60±0.06%, 54.46±0.13%, 83.46±0.29%, 113.54±0.52% and 144.61±0.83%, respectively. While the improvements of the heat extraction per linear meter (HEPM) of

borehole depth are 11.71±0.05 %, 21.94±0.11 %, 31.05±0.20 %, 39.27±0.34 % and 46.77±0.5%, respectively. The above results indicate that the borehole depth has great influence on HECI and HEPM. Deeper borehole means bigger heat exchanger and higher mean borehole wall temperature, therefore HECI and HEPM increase with borehole depth increases.

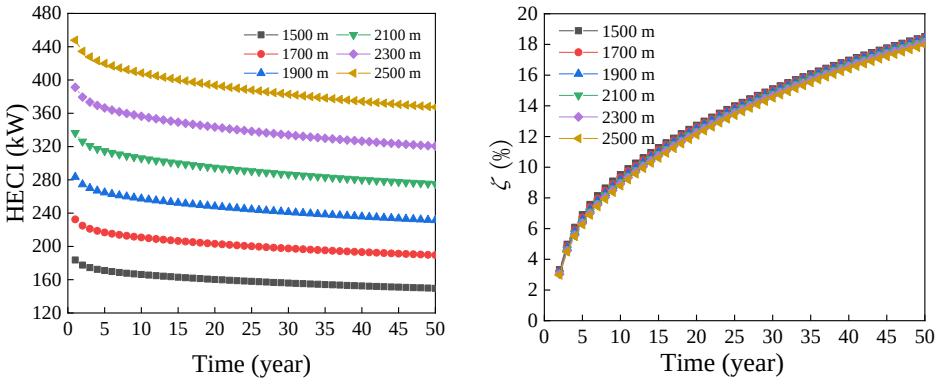

(a) (b)

Fig. 9. Variation of (a) HECI and (b) ζ with different borehole depths.

The influence of borehole depth on the attenuation of heat extraction capacity, i.e. ζ, is shown in **Fig. 9**(b). As shown in **Fig. 9**(b) when the borehole depth ranges in 1500-2500 m, after 10, 20, 30, 40 and 50 years, ζ reaches 9.15±0.36 %, 12.42±0.32 %, 14.81±0.29 %, 16.69±0.28 %, 18.23±0.28 %, respectively. For the temperature of soil adjacent to boreholes goes down year by year due to heat extraction, the HECI of DBHE arrays decreases every year. According to **Eq. (17)**, the ζ gradually increases with operation time extends. However, **Fig. 9**(b) also shows that borehole depth has no significant influence on ζ.

4.5. Influence of soil thermal conductivity on heat extraction capacity and its attenuation

In order to understand the influence of thermal conductivity on the heat extraction capacity of DBHE arrays and simplify the analysis, the underground stratification is ignored. Assume that the geotechnical physical properties are uniform, the volume heat capacity of the soil/rock is 2.5×10^6 J/(m^3·K), the soil thermal conductivities are 1.0 W/(m·K), 1.5 W/(m·K), 2.0 W/(m·K), 2.5 W/(m·K), and 3.0 W/(m·K), respectively. Other parameters are shown in **Table 2** and **Table 3**.

The calculation results of cases with different soil thermal conductivity and same terrestrial heat flow rate are shown in **Fig. 10**.

Fig. 10(a) shows that HECI increases with the increase of soil thermal conductivity when terrestrial heat flow rate is 0.03W/m^2. At the same time, **Fig. 10**(b) shows that when terrestrial heat flow rate is 0.075W/m^2, the HECI decreases with the increase of thermal conductivity. **Fig. 10**(a) and (b) indicates that when the terrestrial heat flow rate is different, the HECI variation versus thermal conductivity may has different trends. The thermal conductivity increase brings two kinds of effects on heat extraction of DBHE arrays. On the one hand, larger thermal conductivity induces better heat conduction in soil, which is conducive to heat extracting. On the other hand, with same terrestrial heat flow rate, larger thermal conductivity means lower borehole bottom temperature according to **Eq. (3)**, which resulting in lower average temperature between circulating fluid and borehole wall and brings negative effect on heat extraction. The influence of thermal conductivity on heat extraction capacity depends on the comprehensive action of the above two aspects.

Fig. 10 (c) and (d) shows that ζ has similar developing trends with different soil thermal

conductivity when other conditions are same, and the influence of thermal conductivity on it is not apparent during the 50-year operation period. After 40 years, the ζ at different soil thermal conductivity is almost the same.

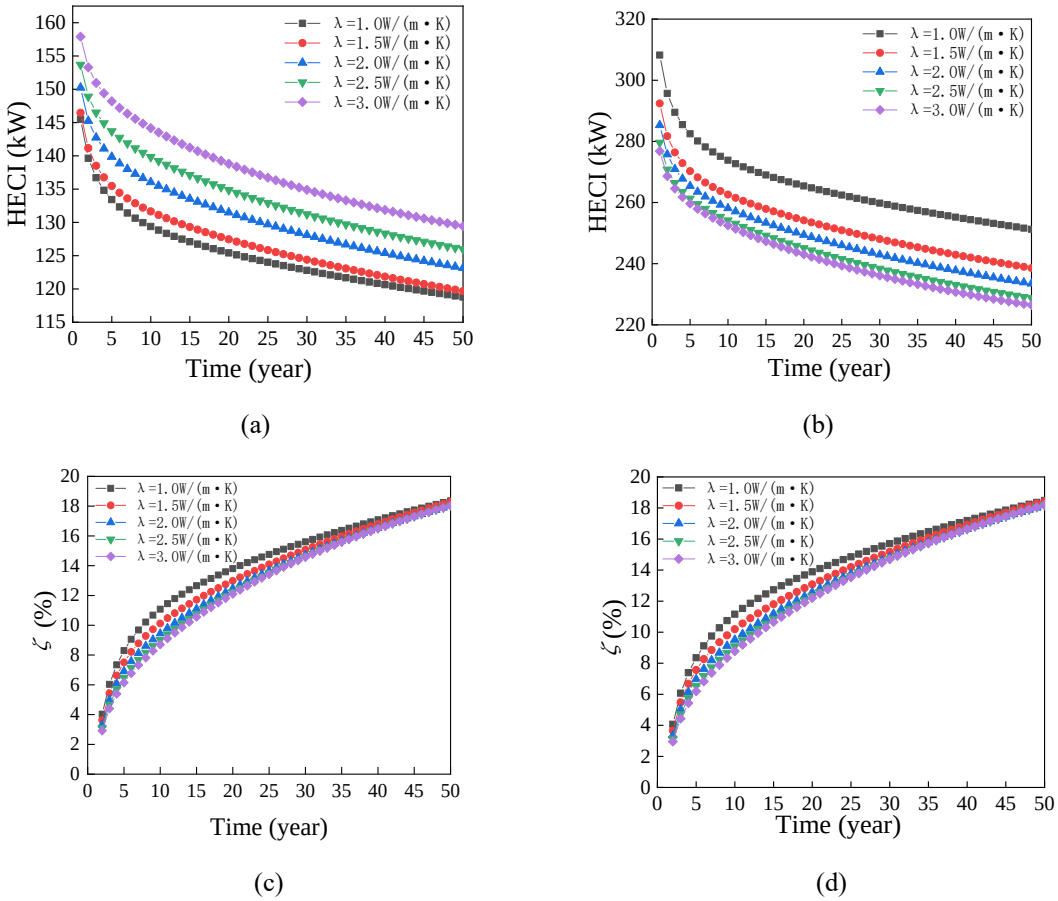

Fig. 10. Variation of HECI with different thermal conductivity when terrestrial heat flow rate is (a) 0.03W/m^2 and (b) 0.075W/m^2, and variation of ζ with different thermal conductivity when terrestrial heat flow rate is (c) 0.03W/m^2 and (d) 0.075W/m^2.

The influence of soil thermal conductivity is also analyzed under the condition with same ground temperature gradient in order to avoid discussing the influence of thermal conductivity on borehole bottom temperature. When the ground temperature gradient is 0.03 ℃/m, and the borehole bottom temperature is 75 ℃, calculation and analysis are carried out according to the cases list in

Table 4 with same geothermal gradients and borehole bottom temperature, the calculation results are shown in **Fig. 11**.

As can be seen from **Fig. 11**(a), when the bottom temperatures of the boreholes are the same, HECI increases with the increase of thermal conductivity and attenuates with the increase of time. Compared with the HECI of Case 1 with thermal conductivity of 1.00 W/(m·K), the change rates of HECIs of Case 2 to Case 5 are 34.80±0.71%, 66.61±1.47%, 94.32±2.15% and 120.30±2.83% respectively. When the borehole bottom temperature is constant, thermal conductivity variation has great influence on HECI. The reason is that terrestrial heat flow rate is proportional to soil thermal conductivity when the borehole bottom temperature is same.

As shown in **Fig. 11**(b), heat extraction attenuation rate ζ increases with time extends, and the influence of thermal conductivity on it is not apparent during the 50-year operation period. After 40 years,

the ζ at different soil thermal conductivity is also almost the same.

Table 4 Five cases with the same borehole bottom temperature.

Case	1	2	3	4	5
Thermal conductivity (W/(m·K))	1.00	1.50	2.00	2.50	3.00
Terrestrial heat flow rate (W/m^2)	0.03	0.045	0.06	0.075	0.09

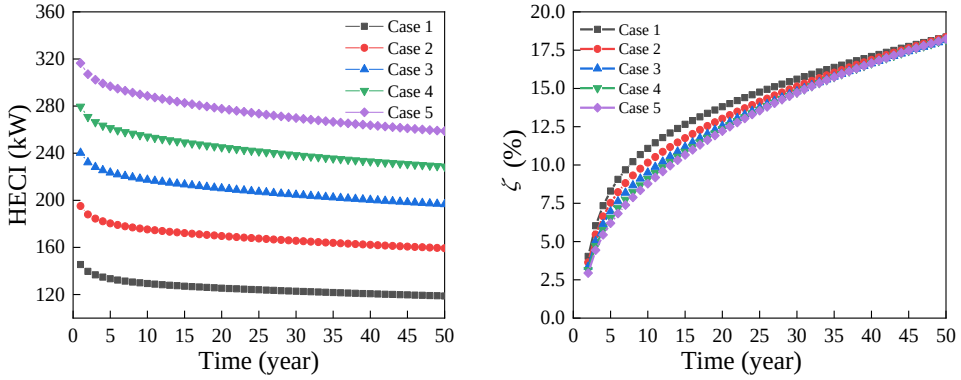

(a) (b)

Fig. 11. Variation of (a) HECI and (b) ζ at the same borehole bottom temperature.

4.6. Influence of pipe size on heat extraction capacity and its attenuation

4.6.1 Influence of outer pipe size

At present, outer pipes of DBHE usually use oil casing. In this section, outer pipe sizes of Φ168.3×8.94, Φ177.8×9.19, Φ193.7×8.33, Φ219.1×10.16 and Φ244.5×10.3 mm are considered based on the specification of oil casing [19]. The inner pipe size is set as Φ110×10 mm. The result is shown in **Fig. 12**.

Fig. 12(a) shows that for all outer pipe sizes, HECI increases with outer pipe diameter increases, and attenuates with time extends. In **Fig. 12**(a), when the outer pipe sizes are 177.8×9.19 mm, 193.7×8.33 mm, 219.1×10.16 mm and 244.5×10.3 mm, compared with the HECI of the DBHE outer pipe size of Φ168.3 ×8.94 mm, the change rate ranges of the HECI during the 50-year operation period are 0.92 ~ 1.16 %, 2.46 ~ 3.06 %, 4.71 ~ 5.86 % and 6.78 ~ 8.50 %, respectively. With increase of the outer pipe size, the heat flow area between the circulating fluid and the outer pipe, and that between the outer pipe and the borehole wall increase. Meanwhile, the grout layer thickness decreases. Therefore, the thermal resistance between the circulating fluid and borehole wall reduces, which is conducive to heat transfer.

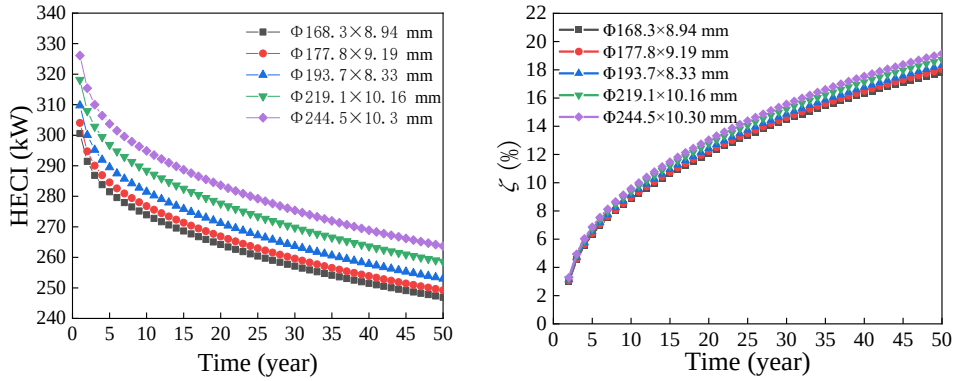

(a) (b)

Fig. 12. Variation of (a) HECI and (b) ζ with different outer pipe sizes.

As shown in **Fig. 12**(b), ζ gradually increases with time. When the outer pipe sizes are Φ168.3×8.94 mm, Φ177.8×9.19 mm, Φ193.7×8.33 mm, Φ219.1×10.16 mm and Φ244.5×10.3 mm, ζ increases to 17.83 %, 18.03 %, 18.31 %, 18.72 % and 19.14 % at the end of the 50-year operation cycle, respectively. With outer pipe size increases, ζ increases, though the increase is not much. As mentioned in the above paragraph that the HECI increases with the outer pipe size increases, which indicates that more heat is drawn from the soil adjacent to boreholes with larger outer pipe when the other conditions are same, therefore the soil temperature decreases much lower and more difficult to restore the geothermal field during non-operation periods. Thus, to some extent, ζ increases with outer pipe size increases.

4.6.2 Influence of inner pipe size

Inner pipe sizes of Φ50×4.6 mm, Φ63×5.8 mm, Φ75×6.8 mm, Φ90×8.2 mm, Φ110×10 mm and Φ125×11.4 mm are considered based on the production specification of polyvinyl chloride pipe. The increase of inner pipe outer diameter and wall thickness have complicated influences on the thermal short circuit between inner and outer pipes. If the inner pipe outer diameter is kept unchanged and the inner pipe wall thickness is increased, the thermal resistance between inner pipe and outer pipe will increase, and the heat extraction capacity of DBHE array will increase. If the inner pipe wall thickness is kept unchanged and the inner pipe outer diameter is increased, the heat transfer area between inner pipe and outer pipe, the fluid velocity in inner pipe and outer pipe will change. At this point, it cannot be simply to say whether the heat extraction capacity increases or decreases with the increase of inner pipe diameter. The influences of inner pipe outer diameter and wall thickness on average borehole HECI of the four-borehole array are shown in **Fig. 13**(a) and (b), respectively.

Fig. 13(a) shows that when the inner pipe wall thickness maintains constant, HECI decreases with the increase of the inner pipe diameter. Compared with the HECI of the case that the inner pipe outer diameter is 50 mm, the HECI of the case that with the inner pipe outer diameter of 125 mm changes by -2.82±0.29% during the 50-year operation period. **Fig. 13**(b) shows that when the inner pipe outer diameter remains unchanged, the greater the inner pipe wall thickness is, the greater the heat extraction capacity of the DBHE array is. Compared to the HECI with the inner pipe wall thickness of 4.6mm, the HECI with inner pipe wall thickness of 11.4 mm increases by 2.80±0.29 % during the 50-year operation.

Fig. 13(c) shows when the DBHE inner pipe adopts the above standard sizes, the HECIs are nearly same, which is consistent with the results shown in **Fig. 13**(a) and **Fig. 13**(b). For standards inner pipes, inner pipe flow area, the pipe wall thickness and inner pipe perimeter increase, and the outer annular tunnel cross area decreases with inner pipe diameter increases. However, fluid velocity in inner pipe decrease induced by inner pipe flow area increase and wall thickness increase make the thermal resistance increases. At the same time, the radial heat flow area increase caused by inner pipe perimeter increase and the fluid velocity in outer pipe increase due to annular tunnel cross area decrease cause thermal resistance decreases. As the result, the total thermal resistance maintains relatively constant when inner pipe size changes as shown in **Table 5**. **Table 5** lists the inner pipe, outer pipe and overall thermal resistance with different standard inner pipe sizes. It shows that the overall borehole thermal resistance is nearly same and the maximum difference is no more than 0.01 m·K/W. Thus, the HECIs are nearly unchanged when the inner pipe size varies.

For all the cases with different standard inner pipe sizes, the HECI variation versus time are nearly same, and also the ζ variation. It can be concluded that HECI and ζ are nearly independent of standard inner pipe sizes.

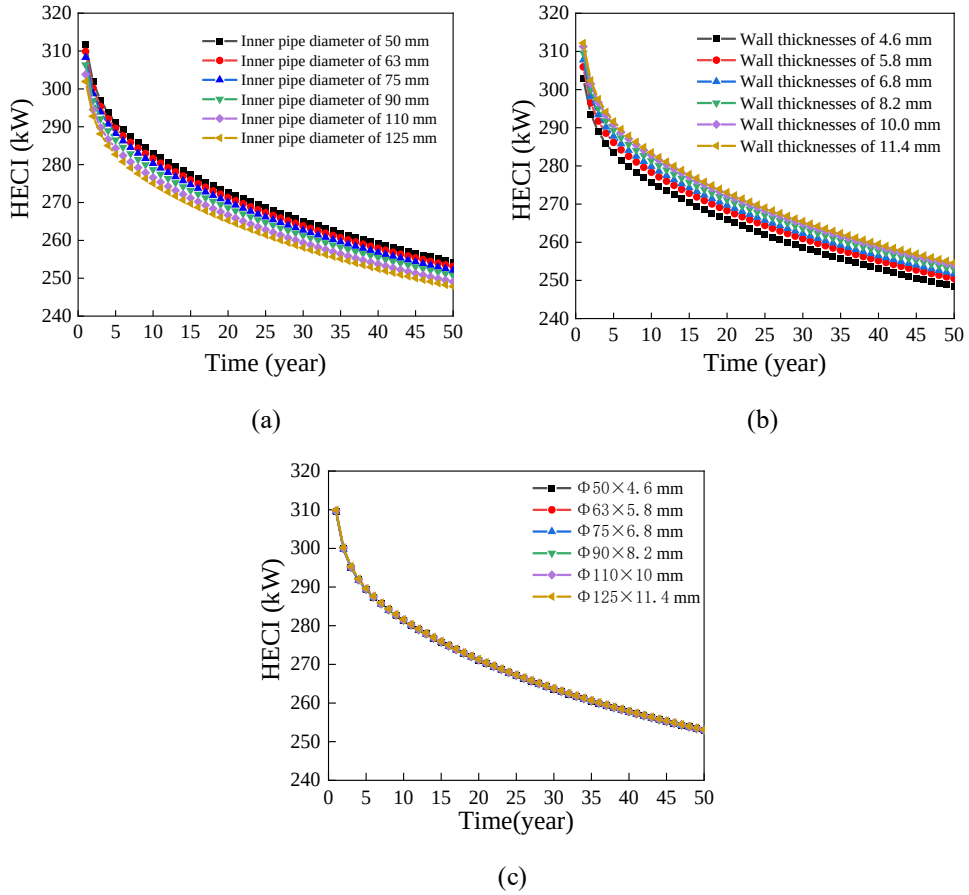

Fig. 13. (a) Variation of HECI with different inner pipe diameters when wall thickness is 6 mm, (b) variation of HECI with different wall thicknesses when inner pipe diameter is 90 mm, and (c) variation of HECI with different inner pipe sizes.

Table 5 The borehole thermal resistance with different inner pipe sizes.

Inner diameter (mm)	Φ50×4.6	Φ63×5.8	Φ75×6.8	Φ90×8.2	Φ110×10	Φ125×11.4
Thermal resistance of inner pipe (m·K/W)	0.081-0.088	0.081-0.085	0.08-0.083	0.08-0.083	0.08-0.082	0.08-0.082
Thermal resistance of outer pipe (m·K/W)	0.036-0.038	0.036-0.037	0.036-0.037	0.036-0.037	0.036-0.037	0.036-0.037
Overall thermal resistance (m·K/W)	0.117-0.126	0.117-0.122	0.116-0.120	0.116-0.120	0.116-0.119	0.116-0.119

4.7 Influence of circulating fluid mass flow rate on heat extraction capacity and its attenuation

As well known, circulating fluid flow rate always has apparent influence on operation performance of heat exchangers. Based on comprehensive consideration of heat transfer efficiency and economy, circulating fluid velocity in DBHEs usually ranges in 0.25m /s ~ 1.00m/s. In this section, the outer pipe size is set as Φ193.7 ×8.33 mm; and the inner pipe size is set as Φ110 ×10 mm. Thus, the corresponding circulating fluid mass flow rate usually ranges in 4.58 kg/s ~ 18.30 kg/s. Therefore, in the following

analysis, mass flow rates are set as 6.0 kg/s, 8.0 kg/s, 10.0 kg/s, 12.0 kg/s, 14.0 kg/s, 16.0 kg/s and 18.0 kg/s. The HECI and ζ of cases with different fluid mass flow rates are calculated and shown in **Fig. 14**.

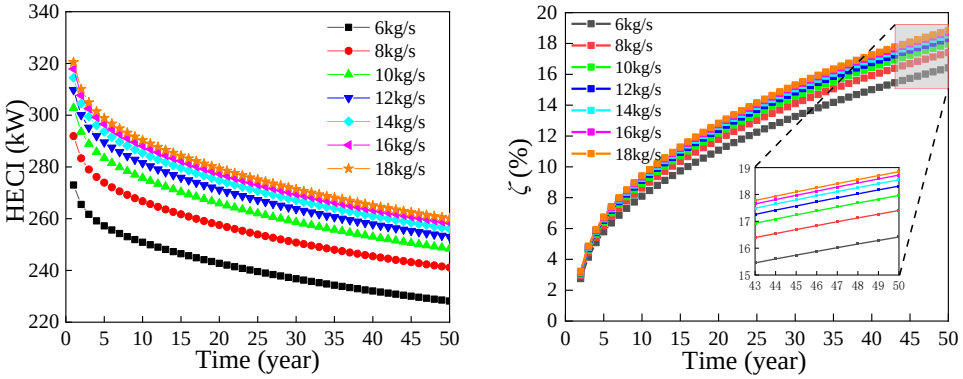

(a) (b)

Fig. 14. Variation of (a) HECI and (b) ζ with different mass flow rates.

As shown in **Fig. 14**(a), for all fluid mass flow rates, the HECI increases with mass flow rate increases and attenuates with time extends. Compared with the HECI with the fluid mass flow rate of 6.0 kg/s, the change rates of HECIs with the fluid mass flow rates of 8.0 kg/s, 10.0 kg/s, 12.0 kg/s, 14.0 kg/s, 16.0 kg/s and 18.0 kg/s during 50 years operation range in 5.67 ~ 6.93 %, 8.86 ~ 10.92 %, 10.88 ~ 13.45 %, 12.25 ~ 15.19 %, 13.23~ 16.44 % and 13.97 ~ 17.39 %, respectively. For a given pipe, the thermal convection coefficient increases with mass flow rate increases, which promotes the heat transfer between the fluid and pipe wall. Hence, HECI increases with fluid flow rate increases. However, **Fig. 14**(a) also shows that HECI improvement caused by increasing fluid mass flow rate is not unlimited. When the fluid mass flow rate is larger than 10 kg/s, the HECI increment induced by improving the mass flow rate is not much yet.

Fig. 14(b) shows that ζ increases with the fluid mass flow rate increases. The reason is as same as mentioned in above section. When the fluid mass flow rate increases, HECI increases and causes the soil temperature decreases more lower and more difficult to restore the geothermal field during non-operation periods. Therefore, ζ increases with the fluid mass flow rate increases. **Fig. 14**(b) also shows that, when the fluid mass flow rate is large enough (larger than 10 kg/s), the difference of ζ between cases with different fluid mass flow rate is not much.

5. Conclusions

(1) Based on the superposition principle, a dimension reduction algorithm is proposed to decompose the complex three-dimensional heat transfer problem of DBHE arrays into the superposition of several single-borehole two-dimensional problems in cylindrical coordinate. By this way, the calculation workload of DBHE arrays heat transfer problem is greatly reduced. The software of FLUENT is used to verify the proposed algorithm. The verification shows that the dimension reduction algorithm is highly consistent with the calculation results of the FLUENT software with almost the same accuracy, and the numerical calculation speed has been improved by several orders of magnitude.

(2) The thermal interference among boreholes decreases with the increase of borehole spacing, which is beneficial to improving the heat extraction capacity of DBHEs. When the borehole spacing is larger than 40 m, if the DBHE arrays service lifetime is no more than 50 years, the per borehole heat extraction capacity of the four-borehole DBHE is not quite different from that of the single-borehole DBHE, and the maximum gap is no more than 10 % in the whole service life.

(3) The thermal extraction capacity and its attenuation characteristics of DBHE arrays are explored. The results show that borehole spacing, annual heating duration and total operation time significantly affect HECI and ζ of DBHE arrays. When other conditions are fixed, borehole spacing decrease, annual heating duration increase and service life extension will induce the HECIs decrease and ζ increase. When the annual heating duration is 4 months and the service life is 50 years, if the borehole spacing increases from 20 m to 70 m, compared with the HECI of the single-borehole DBHE, the decrease of the per borehole HECI of the four-borehole DBHE will change from -17.03 % to-2.62 %, and ζ will decrease from 28.08 % to 15.59 % .When the borehole spacing of is 50 m and the service life is 50 years, if the annual heating duration increases from 4 to 6 months, the HECI of the four-borehole DBHE will decrease by 11.0 %, and ζ will increase from 18.31 % to 24.33 %. When the annual heating duration is 6 months and the borehole spacing is 50 m, if the service life increases from 20 to 50 years, the HECI of the four-borehole DBHE will decrease by 9.0 % and the ζ will increase from 12.43% to 18.31%.

(4) The terrestrial heat flow rate, borehole depth, outer pipe size and fluid flow rate have significant effects on HECI, in which terrestrial heat flow rate and borehole depth have even greater effects on HECI, but less on ζ. When the service life is 50 years and the terrestrial heat flow rate increases from 0.03 W/m^2 to 0.09 W/m^2, the corresponding HECI increases 127.6 %, but the maximum ζ difference between the cases with different service life is less than 0.07 %. When the service life is 50 years and the borehole depth increased from 1500 m to 2,500 m, the HECI increases 144.61 %, but maximum ζ difference between the cases with different depth is less than 0.36 %.

(5) On the premise of constant terrestrial heat flow rate and borehole depth, HECI may increase or decrease with the increase of soil thermal conductivity. The reason is that when the soil thermal conductivity increases, the soil heat conduction is enhanced, which has positive influence on HECI, while the borehole bottom temperature decreases, which has negative effects on HECI. When the borehole depth and bottom temperature are constant, HECI increases with the increase of the soil thermal conductivity. This is due to the terrestrial heat flow rate and the soil heat conduction increase with soil thermal conductivity increases.

(6) For standard outer pipe of DBHE, HECI increases with the diameter increases. the main reason is that the heat flow area between the circulating fluid and the outer pipe, and that between the outer pipe and the borehole wall increase with the increase of the outer pipe diameter, which reduces the thermal resistance between the circulating fluid and borehole wall. Though the ζ increases with outer pipe size increases, the increase range is not large. The inner pipe size has little effect on HECI and ζ. This is because when its size changes, some thermal resistance increases while others decrease, which causes the total thermal resistance of borehole almost unchanged.

Acknowledgement

This work was financially supported by the Natural Science Foundation of Shandong Province, China [No. ZR2020ME219]; and Leading Researcher Studio Fund of Jinan [No. 2019GXRC066].

References

[1] Nian YL, Cheng WL, Yang XY, Xie K. Simulation of a novel deep ground source heat pump system using abandoned oil wells with coaxial BHE. International Journal of Heat and Mass Transfer 2019; 137: 400-12.

[2] Zhang Y, Wang X, Xue Y, Wang F, Guan Y, Zhou C. The key heating technology of "water

retention and heat extraction" for deep geothermal energy development in Guanzhong Basin. District Heating 2020; 4: 122-8.
[3] Wang F, Cai W, Wang M, Gao Y, Liu J, Wang Z, Xu H. Status and outlook for research on geothermal heating technology. Journal of Refrigeration 2021; 42(1): 14-22.
[4] Luo Y, Yu J, Yan T, Zhang L, Liu X. Improved analytical modeling and system performance evaluation of deep coaxial borehole heat exchanger with segmented finite cylinder-source method. Energy & Buildings 2020; 212:109829.
[5] Luo Y, Guo H, Meggers F, Zhang L. Deep coaxial borehole heat exchanger: Analytical modeling and thermal analysis. Energy 2019; 185: 1298-313.
[6] Beier RA, Acuña J, Mogensen P, Palm B. Transient heat transfer in a coaxial borehole heat exchanger. Geothermics 2014; 51: 470-82.
[7] Li C, Guan Y, Wang X, Li G, Zhou C, Xun Y. Experimental and numerical studies on heat transfer characteristics of vertical deep-buried U-bend pipe to supply heat in buildings with geothermal energy. Energy 2018; 142: 689-701.
[8] Renaud T, Verdin P, Falcone G. Numerical simulation of a Deep Borehole Heat Exchanger in the Krafla geothermal system. International Journal of Heat and Mass Transfer 2019; 143:118496.
[9] Cai W, Wang F, Chen S, Chen C, Liu J, Deng J, Kolditz O, Shao H. Analysis of heat extraction performance and long-term sustainability for multiple deep borehole heat exchanger array: A project-based study. Applied Energy 2021; 289:116590.
[10] Kong Y, Chen C, Shao H, Pang Z, Xiong L, Wang J. Principle and capacity quantification of deep-borehole heat exchangers. Chinese Journal of Geophysics 2017; 60(12): 4741-52.
[11] Bär K, Rühaak W, Welsch B, Schulte D, Homuth S, Sass I. Seasonal High Temperature Heat Storage with Medium Deep Borehole Heat Exchangers. Energy Procedia 2015; 76: 351-60.
[12] Welsch B, Rühaak W, Schulte DO, Bär K, Sass I. Characteristics of medium deep borehole thermal energy storage. International Journal of Energy Research 2016; 40(13): 1855-68.
[13] Holmberg H, Acuña J, Næss E, Sønju OK. Thermal evaluation of coaxial deep borehole heat exchangers. Renewable Energy 2016; 97: 65-76.
[14] Fang L, Diao N, Shao Z, Zhu K, Fang Z. A computationally efficient numerical model for heat transfer simulation of deep borehole heat exchangers. Energy & Buildings 2018; 167: 79-88.
[15] Cai W, Wang F, Liu J, Wang Z, Ma Z. Experimental and numerical investigation of heat transfer performance and sustainability of deep borehole heat exchangers coupled with ground source heat pump systems. Applied Thermal Engineering 2019; 149: 975-86.
[16] Yu M, Lu W, Zhang F, Zhang W, Cui P, Fang Z. A novel model and heat extraction capacity of mid-deep buried U-bend pipe ground heat exchangers. Energy & Buildings 2021; 235:110723.
[17] Deng J, Wei Q, Liang M, He S, Zhang H. Field test on energy performance of medium-depth geothermal heat pump systems (MD-GHPs). Energy & Buildings 2019; 184: 289-99.
[18] Li J, Xu W, Li J, Huang S, Li Z, Qiao B, Yang C, Sun D, Zhang G. Heat extraction model and characteristics of coaxial deep borehole heat exchanger. Renewable Energy 2021; 169: 738-51.
[19] Liu J, Wang F, Gao Y, Zhang Y, Cai W, Wang M, Wang Z. Influencing factors analysis and operation optimization for the long-term performance of medium-deep borehole heat exchanger coupled ground source heat pump system. Energy & Buildings 2020; 226:110385.
[20] Ran Y, Bu X. Simulation study on rock temperature characteristics of single well geothermal heating system. Advances in New and Renewable Energy 2019; 7(2): 161-7.

[21] Zhang F, Fang L, Jia L, Man Y, Cui P, Zhang W, Fang Z. A dimension reduction algorithm for numerical simulation of multi-borehole heat exchangers. Renewable Energy 2021; 179: 2235-45.
[22] Fang Z, Diao N, Cui P. Discontinuous operation of geothermal heat exchangers. Tsinghua Science and Technology 2002; 7(2): 194-7.
[23] Walch A, Mohajeri N, Gudmundsson A, Scartezzini JL. Quantifying the technical geothermal potential from shallow borehole heat exchangers at regional scale. Renewable Energy 2021; 165: 369-80.
[24] Huang Y, Zhang Y, Xie Y, Zhang Y, Gao X, Ma J. Long-term thermal performance analysis of deep coaxial borehole heat exchanger based on field test. Journal of Cleaner Production 2021; 278:123396.
[25] Chen S, Cai W, Witte F, Wang X, Wang F, Kolditz O, Shao H. Long-term thermal imbalance in large borehole heat exchangers array – A numerical study based on the Leicester project. Energy & Buildings 2021; 231:110518.
[26] Wang J, et al. Geothermics and Its Applications. 1st ed. Beijing: Science Press; 2015.